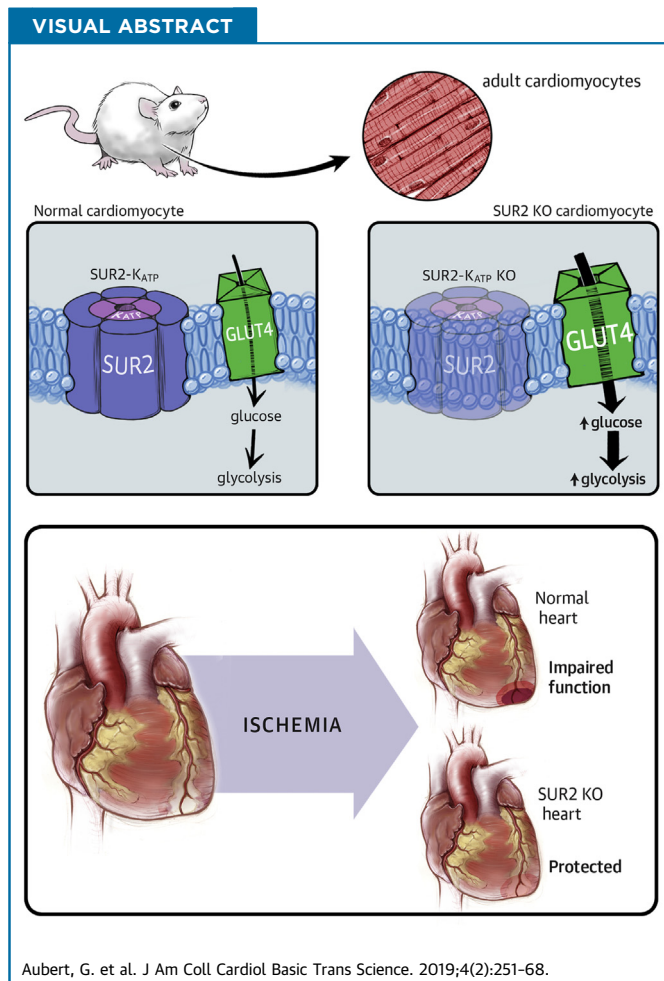


PRECLINICAL RESEARCH

Deletion of Sulfonylurea Receptor 2 in the Adult Myocardium Enhances Cardiac Glucose Uptake and Is Cardioprotective



Gregory Aubert, MD, PhD,^{a,*} David Y. Barefield, PhD,^{a,*} Alexis R. Demonbreun, PhD,^{a,*} Mohun Ramratnam, MD,^{b,*} Katherine S. Fallon, BS,^a James L. Warner, BA,^a Ann E. Rossi, PhD,^c Michele Hadhazy, BS,^a Jonathan C. Makielski, MD,^b Elizabeth M. McNally, MD, PhD^c



From the ^aCenter for Genetic Medicine, Northwestern University Feinberg School of Medicine, Chicago Illinois; ^bDivision of Cardiology, Department of Medicine, University of Wisconsin-Madison, Madison, Wisconsin; and the ^cSection of Cardiology, University of Chicago, Chicago Illinois. *Drs. Aubert, Barefield, Demonbreun, and Ramratnam contributed equally to this work and are joint first authors. Supported by National Institutes of Health Grant No. HL 122109. The funders had no role in determining the experimental design or results interpretation. Dr. McNally has served as a consultant for Exonics, AstraZeneca, and Invitae;

ABBREVIATIONS
AND ACRONYMS**2DG** = 2-deoxy-D-glucose**EDTA** = ethylenediaminetetraacetic acid**FL Ex5** = LoxP sites flanking exon 5**GFP** = green fluorescent protein**GLUT** = glucose transporter**HEK293T** = human embryonic kidney 293T**K_{ATP}** = adenosine triphosphate-sensitive potassium**Kir** = inward rectifying potassium channel**LVDP** = left ventricular developed pressure**MCM** = α MHC-MerCreMer**PCR** = polymerase chain reaction**SUR** = sulfonylurea receptor

SUMMARY

The adult myocardium relies on oxidative metabolism. In ischemic myocardium, such as the embryonic heart, glycolysis contributes more prominently as a fuel source. The sulfonylurea receptor 2 (SUR2) was previously implicated in the normal myocardial transition from glycolytic to oxidative metabolism that occurs during adaptation to postnatal life. This receptor was now selectively deleted in adult mouse myocardium resulting in protection from ischemia reperfusion injury. SUR2-deleted cardiomyocytes had enhanced glucose uptake, and SUR2 forms a complex with the major glucose transporter. These data identify the SUR2 receptor as a target to shift cardiac metabolism to protect against myocardial injury. (J Am Coll Cardiol Basic Trans Science 2019;4:251-68) © 2019 The Authors. Published by Elsevier on behalf of the American College of Cardiology Foundation. This is an open access article under the CC BY-NC-ND license (<http://creativecommons.org/licenses/by-nc-nd/4.0/>).

Adenosine triphosphate-sensitive potassium (K_{ATP}) channels respond to intracellular adenosine diphosphate-ATP ratio (1-4). In excitable cells and states where adenosine diphosphate is high, K_{ATP} channels open, allowing potassium efflux and cellular hyperpolarization. Correspondingly, high-ATP states promote K_{ATP} channel closure and cellular depolarization.

Changes in membrane potential trigger a cascade of responses including the opening of voltage-sensitive calcium channels accompanied by an increase in intracellular calcium and shortening of the action potential to make the heart energetically more efficient (5,6). K_{ATP} channels contain 2 subunits, an inwardly rectifying potassium ion channel (Kir) (Kir6.1 or Kir6.2) and the sulfonylurea receptor (SUR1 or SUR2) (7-10). SUR2-containing K_{ATP} channels are enriched in the heart, skeletal muscle, and vascular smooth muscle, where they regulate a range of physiological effects including cardiac stress response, blood pressure, and vascular tone (2). The major ventricular cardiomyocyte K_{ATP} channel is composed of SUR2 and Kir6.2, encoded by *ABCC9* and *KCNJ11*, respectively. In the mouse, genetic deletion of Kir6.2 leads to calcium overload and myocardial damage (5). Loss of Kir6.2 also leads to enhanced myocardial damage in the setting of hypertension and toxemia (11,12). Taken together, these studies describe enhanced susceptibility to stress in the cardiomyocyte lacking the Kir component of functional K_{ATP} channels.

We previously generated and characterized mice with 2 different deletions in SUR2. The first was a global deletion in which exons 14 to 18 of *Abcc9* were removed (13). These exons encode the first nucleotide-binding domain of SUR2 and with this deletion no full-length protein was detectable. This model, now referred to as SUR2-Ex14/18, developed hypertension, episodic coronary artery vascular spasm, bradycardia, and sudden death (13). Deleting *Kcnj8*, which encodes Kir6.1 and is the major component of vascular smooth muscle K_{ATP} channels, induced a similar phenotype (14). The similar phenotype between Kir6.1 and SUR2-deleted mice supported the notion that vascular spasm arises from loss of SUR2-Kir6.1 K_{ATP} channels in vascular smooth muscle.

The physiological role of SUR2-K_{ATP} channels is complex. Although loss of SUR2 results in vascular spasm and sudden death, it was also associated with protection from ischemic insult in surviving animals (15). SUR2 Ex14/18 mice were found to have reduced infarct size after global ischemia compared with normal mice, and therefore, protection from ischemia occurred in the absence of SUR2-K_{ATP} channels. We hypothesized that the continual vasospasm present in these animals was sufficient to trigger a preconditioned-like myocardium that was more resistant to stress. An alternative hypothesis implicated a smaller protein produced from the *Abcc9* gene, called SUR2-55, as responsible for mediating cardiac protection (16,17). SUR2-55 remained intact

and is a founder of Ikaika Therapeutics. All other authors have reported that they have no relationships relevant to the contents of this paper to disclose.

All authors attest they are in compliance with human studies committees and animal welfare regulations of the authors' institutions and Food and Drug Administration guidelines, including patient consent where appropriate. For more information, visit the JACC: Basic to Translational Science [author instructions page](#).

Manuscript received October 19, 2018; revised manuscript received November 24, 2018, accepted November 26, 2018.

and readily detectable in SUR2-Ex14/18 mice. To assess this hypothesis, we generated a distinct deletion strategy for *Abcc9* to ablate both full-length SUR2 and SUR2-55. This mouse model, SUR2-Ex5, died in the neonatal window with cardiomyopathy, further suggesting a critical role for SUR2-55 in cardiac adaptation to postnatal life (18). We specifically found that SUR2-Ex5 mice failed to normally transition from glycolytic metabolism that is present in fetal myocardium to the postnatal oxidative metabolic state (18).

To address the role of SUR2 in the adult myocardium, we generated adult mice with a conditional ablation of *Abcc9*/SUR2 in the ventricular myocardium. These mice, referred to as cardiac-deleted SUR2 mice, survive with a mild reduction in left ventricular function. Cardiac-deleted SUR2 mice displayed protection from myocardial ischemia and augmented cardiomyocyte glucose handling. We found that SUR2 interacts with glucose transporter 4 (GLUT4), the major insulin-responsive glucose transporter in the adult cardiomyocyte. Correspondingly, SUR2-deleted cardiomyocytes had increased glycolysis. Taken together, these data present a model in which a myocardium favoring glucose metabolism may be better able to survive episodes of ischemic insult.

METHODS

ANIMALS. Mice with *LoxP* sites flanking exon 5 (F1 Ex5) of the *Abcc9* gene were generated by homologous recombination in mouse embryonic stem cells followed by transplantation into a pseudopregnant female. F1 Ex5 mice were crossed with the α MHC-*MerCreMer*⁺ mouse line (Jackson B6.FVB(129)-*A1c*^{fTg(Myh6-cre/Esr1*)1Jmk/J}) and maintained in a hemizygous state (19). These mice were bred and maintained on a C57BL/6J background. Animals were bred at Northwestern University and a subset was shipped to University of Wisconsin. Mice at both institutions were housed in environmentally controlled conditions in a specific pathogen free facility. All animals were housed and treated in accordance with the standards set by the Animal Care and Use Committees at Northwestern University and the University of Wisconsin-Madison.

TAMOXIFEN TREATMENT. Eight-week-old mice were treated via intraperitoneal injection with 50 μ l of 50 mg/ml tamoxifen (T5648, Sigma-Aldrich, St. Louis, Missouri) diluted in sterile sunflower seed oil (S5007, Sigma-Aldrich) and passed through a 0.2- μ m syringe filter. Tamoxifen was administered for 4 consecutive days to cause genomic recombination and deletion of

Abcc9 exon 5. Male and female mice were analyzed 2 to 4 weeks post-injection.

ECHOCARDIOGRAPHY. Cardiac function was assessed by echocardiography conducted under anesthesia (1% vaporized isoflurane in 100% O₂, 0.8 l/min). Echocardiography was performed using a Visual Sonics Vevo 2100 imaging system with an MS550D 22- to 55-MHz solid-state transducer (FujiFilm, Toronto, Canada). Short-axis M-mode images were acquired for analysis to provide heart chamber dimensions and calculate percent fractional shortening. Acquisition and analysis were conducted blinded to genotype.

TELEMETRY. Wireless cardiac TA11 ETA-F10 telemeters (Data Science International, Minneapolis, Minnesota) were surgically implanted subcutaneously in mice anesthetized with 3% vaporized isoflurane. The mice were allowed to recover for 3 days before data collection. Mice were housed individually and overnight electrocardiography recording were taken from 30 min of data when all animals showed clean traces. Mice were injected with 4 mg/kg isoproterenol intraperitoneally in phosphate-buffered saline and telemetric data was acquired for 30 min following the injection. Electrocardiography interval data were averaged for the duration of the recording with 1 average value reported per animal, as previously described (20).

ISOPROTERENOL CHALLENGE. To provide an alternate cardiac insult in vivo, we performed a chronic high-dose isoproterenol challenge (200 mg/kg intraperitoneally) twice daily for 6 days. This protocol has been shown to cause cardiomyocyte injury with minimal hypertrophic remodeling and regeneration (21). Animals were assessed for cardiac function with echocardiography 1 day before and 2 days after completion of the 6-day protocol, followed by sacrifice and tissue collection.

ISOLATED PERFUSED HEART ISCHEMIA AND REPERFUSION EXPERIMENTS. Male mice were anesthetized with inhaled 3% isoflurane and then euthanized with cervical dislocation. Hearts were rapidly excised and placed in chilled heparinized modified Krebs-Henseleit buffer (118-mM NaCl, 4.7-mM KCl, 1.2-mM MgSO₄, 1.2-mM KH₂PO₄, 25-mM NaHCO₃, 2.5-mM CaCl₂, 0.5-mM ethylenediaminetetraacetic acid [EDTA], and 5-mM glucose). Extracardiac tissue was dissected and discarded while the aorta was located. The aorta was then cannulated with the use of a 22-gauge cannula. The cannula was secured in place with 6-0 silk suture. Hearts were then perfused at a constant pressure of 80 mm Hg on a homemade Langendorff apparatus with modified Krebs-Henseleit

buffer that was equilibrated with 95% O₂ and 5% CO₂ at 37°C. The left atrium was then excised and a fluid-filled balloon catheter constructed from a commercially available kit (Harvard Apparatus, Holliston, Massachusetts) was placed in the left ventricle. The balloon catheter was attached to an APT300 pressure transducer (Harvard Apparatus) and baseline left ventricular pressure was set between 5 and 10 mm Hg. Baseline cardiac function was recorded for 30 min. Mice were then subjected to 2 IR injury protocols. Protocol #1 subjected mice to 30 min of ischemia followed by 60 of reperfusion and protocol #2 subjected mice to 45 min of ischemia and 60 min of reperfusion. Hearts were paced at 360 beats/min via epicardial pacing leads with a Grass SD9 stimulator (Grass Instruments, West Warwick, Rhode Island). Left ventricular pressure was recorded throughout the experimental protocol and analyzed using LabChart Pro (ADInstruments, Colorado Springs, Colorado). Upon completion of reperfusion, hearts were rapidly removed from the Langendorff apparatus and perfused with 30 mM of KCl solution to arrest the hearts in diastole. Then the hearts were stained with 1% tetrazolium chloride solution for 10 min. The hearts were then sectioned into 7 to 8 slices. The sections were placed in 10% formalin and photographed the following day for the quantification of infarct size. Percent recovery was calculated by normalizing each time point against the baseline value. Hearts not meeting quality control (spontaneous beating, excessive baseline arrhythmias, or inability to develop a left ventricular (LV) pressure of >60 mm Hg when not paced) were removed (n = 1 heart).

CARDIOMYOCYTE ISOLATION. Mice were treated with 50 U heparin intraperitoneally 20 min before sacrifice. Mice were anesthetized under 5% vaporized isoflurane mixed with 100% oxygen. A thoracotomy was performed and the heart and lungs rapidly excised and submerged into ice-cold Tyrode solution without calcium (143-mM NaCl, 2.5-mM KCl, 16-mM MgCl₂, 11-mM glucose, 25-mM NaHCO₃, pH adjusted to 7.4). The ascending aorta was dissected out of the surrounding tissue and cannulated with an animal feeding needle (7900, Cadence Science, Staunton, Virginia) and secured with a 6-0 silk suture. The heart was initially perfused with 1 ml of ice-cold calcium-free Tyrode solution before being transferred to a Langendorff apparatus (Radnoti, Covina, California). Hearts were perfused with 37°C calcium-free Tyrode solution using a constant pressure (65-cm vertical distance between the buffer reservoir and cannula tip) for 1 to 2 min before perfusion for 5.5 min with digestion solution (0.15% collagenase type 2 [Worthington Biochemical, Lakewood, New Jersey], 0.1% 2,3-butanedione

monoxime, 0.1% glucose, 100-U/ml penicillin/streptomycin, 112-mM NaCl, 4.7-mM KCl, 0.6-mM KH₂PO₄, 40-μM CaCl₂, 0.6-mM Na₂HPO₄, 1.2-mM MgSO₄, 30-μM phenol red, 21.4-mM NaHCO₃, 10-mM HEPES, and 30-mM taurine; pH adjusted to 7.4). The heart was removed from the cannula, triturated with a transfer pipette, and filtered through a 100-μm cell strainer. Cardiomyocytes were allowed to pellet by gravity for 7 min, followed by aspiration of digestion media and washing with stop buffer (formulated identically to digestion solution except with no collagenase and with 1% bovine serum albumin). Cells were again allowed to gravity pellet followed by a wash in stop buffer without bovine serum albumin. Cardiomyocytes were tolerated to calcium by adding Tyrode buffer with 0.3-mM CaCl₂ dropwise. Cell culture dishes were coated with 20 μg/ml laminin (23017-015; Gibco, Thermo Fisher Scientific, Waltham, Massachusetts) for 1 h at room temperature. Laminin solution was aspirated followed by plating of cardiomyocytes for 1 h to allow cell adhesion before experimentation.

POLYMERASE CHAIN REACTION AND GENOMIC DNA ANALYSIS. Genomic DNA was isolated from mouse tail tissues or total myocardial tissue samples. Polymerase chain reaction (PCR) was performed using primers flanking and within *Abcc9* exon 5 (forward primer: 5'-ATGTTGCTCCTTGTTTAA TTCATGC-3'; reverse primer 1: 5'-GTTCTAGAGAGTTCTCCATTCCGTTTG-3'; reverse primer 2: 5'-CGTTGCCAGTTAGAAAGTCAAAGTTAA-3') and amplified using PCR with cycle conditions: 94°C, 30 s; 55°C, 60 s; 72°C, 60 s. Products were run on 2% agarose gel with ethidium bromide to visualize DNA recombination.

REVERSE TRANSCRIPTASE PCR AND QUANTITATIVE PCR ANALYSIS. Ribonucleic acid (RNA) was isolated from whole heart tissue and isolated cardiomyocytes. Samples were immediately placed in TRIzol (Ambion Diagnostics, Austin, Texas) and disrupted using a bead homogenizer (BioSpec, Bartlesville, Oklahoma), followed by centrifugation for 3 min at 12,000 × g at 4°C. Supernatant was mixed with one-fifth volume of chloroform and the tubes were incubated for 5 min at room temperature with periodic shaking, followed by centrifugation for 15 min at 12,000 × g at 4°C. RNA was extracted from the upper aqueous phase. RNA extraction was performed using the Aurum Total RNA Mini Kit (Bio-Rad Laboratories, Hercules, California) with DNaseI digestion, following the manufacturer's guidelines. Complementary DNA was synthesized using qScript cDNA SuperMix (Quanta Biosciences, Gaithersburg, Maryland) from 1 μg of RNA per sample, following the manufacturer's guidelines. Reverse

transcriptase PCR was performed on *Abcc9* to detect the removal of exon 5 from the messenger RNA using primers recognizing exon 4 and the exon 6/7 junction (forward: 5'-GTGCAAATTCATCATAACACGTG-3'; reverse: 5'-CATATCTTCTGACCCGGATGAC-3'). For all reactions, 35 cycles were performed with annealing at 63°C for 30 s and extension at 72°C for 1 min.

Quantitative PCR was performed using iTaq universal SYBR Green supermix (Bio-Rad) in a CFX96 Real-Time PCR Detection System (Bio-Rad). Control reactions were performed with RNA processed using the same method but without reverse transcriptase. Total *Abcc9* expression was assessed using primers designed against the exon 40/3'UTR junction (forward: 5'-TCATTCTCTGCATCGGGTTCAC-3'; reverse: 5'-GACGGTAGGCATTGAAGTACTTG). *Gapdh* was used as the reference gene for normalization (forward: 5'-TTGTGATGGGTGTGAACCACGA-3'; reverse: 5'-AGCCCTCCACAATGCCAAAGT-3'). All quantitative PCR primer sequences are listed in [Supplemental Table 1](#). For all reactions, 40 cycles were performed with annealing and extension at 60°C for 70 s total. Melt curves of the reaction products were obtained for each primer set using SybrGreen master mix. Quantitative PCR data were analyzed using the $\Delta\Delta C_q$ method.

FASTING AND INSULIN CHALLENGE. Mice were fasted for 5 h, during which water was available. Mice were injected with sterile saline as control (minus insulin) or 2 mU/g insulin via intraperitoneal injection. Mice were sacrificed 30 or 60 min post-insulin injection and tissues were immediately harvested. For the 0-min time point, mice were only fasted.

CELL CULTURE. Human embryonic kidney 293T (HEK293T) cells were obtained from ATCC (CRL-11268, American Type Culture Collection, Manassas, Virginia). Cells were grown in Dulbecco's modified Eagle media supplemented with 10% fetal bovine serum and 1% penicillin/streptomycin (Thermo Fisher Scientific, Waltham, Massachusetts) in a 37°C incubator with 5% CO₂.

TRANSFECTIONS. Cultured HEK293T cells were transfected with Glut4-myc (MR208202, OriGene, Rockville, Maryland) and either SUR2-green fluorescent protein (GFP), SUR55-GFP, or KIR6.2-GFP using FuGENE HD transfection reagent (Promega, Madison, Wisconsin). Cells were lysed 24 h post-transfection.

COIMMUNOPRECIPITATION. Cultured HEK293T cells were rinsed once with ice-cold phosphate buffered saline and lysed with radioimmunoprecipitation assay buffer (89900, Thermo Fisher Scientific, Rochester, New York) supplemented with polymethanesulfonyl fluoride- and EDTA-free protease inhibitor cocktail

tablets (11836170001, Roche, Indianapolis, Indiana). Cells were scraped from the plate with a chilled cell-scraper (08-100-241, Thermo Fisher Scientific) and transferred to Eppendorf tubes on ice. Lysates were vortexed and triturated with an insulin syringe (14-829-1A, Thermo Fisher Scientific). Whole hearts were homogenized in radioimmunoprecipitation assay buffer supplemented with polymethanesulfonyl fluoride- and EDTA-free protease inhibitor cocktail tablets using a Dounce tissue grinder. Lysates were centrifuged at 10,000 × g for 5 min at 4°C and the supernatant was stored at -80°C until use; 500-μg protein (cells) or 1,000-μg protein (tissue) was cleared by nutating with 75-μl protein A/G beads (IPO5, Millipore, Burlington, Massachusetts) and resuspended in lysis buffer for 1 h at 4°C. Cleared lysates were incubated with 3-μg anti-myc antibody (cells), 3-μg anti-Glut4 (tissue), or rabbit immunoglobulin G (31235, Thermo Fisher Scientific) for 3 h at 4°C on a nutator, followed by addition of 50-μl protein A/G beads and another 3-h incubation on a nutator at 4°C. Beads were washed 3 times with lysis buffer and centrifuged at 1000 × g for 1 min. Following the final wash, sample was eluted by addition of 25 μl of 2× Laemmli sample buffer (161-0737, Bio-Rad) with β-mercaptoethanol and incubated at room temperature for 30 min, 15 μl of urea buffer was then added before the sample was pipetted off the beads and stored at -20°C before being analyzed by sodium dodecyl sulfate polyacrylamide gel electrophoresis.

PROTEIN ISOLATION. Hearts were harvested and flash-frozen. TES buffer (20-mmol/l Tris, 250-mmol/l sucrose, 1-mmol/l EDTA, pH 7.4) with 1× complete protease (4693132001, Sigma-Aldrich) and phosphatase inhibitor tablets (4906837001, Sigma-Aldrich) was used for protein homogenization in a bead beater tissue homogenizer (BioSpec). Homogenized tissue samples were heated to 70°C in 2× Laemmli and ran on a 4% to 15% TGX gel (Bio-Rad).

MICROSOME PREPARATION. Total cardiac muscle membranes were prepared from age-matched mice using a protocol modified from (22,23). Hearts were excised, washed in phosphate buffered saline, and minced. Tissue was incubated in 1 ml high salt solution (2-mol/l NaCl, 20-mmol/l HEPES, pH 7.4, 5-mmol/l Na₃) for 30 min at 4°C, centrifuged for 5 min at 1000 × g at 4°C, and the supernatant was discarded. The pellet was homogenized in 6 ml of TES buffer (20-mmol/l Tris, 250-mmol/l sucrose, 1-mmol/l EDTA, pH 7.4) using a Dounce homogenizer. The homogenate was centrifuged for 5 min at 1000 × g at 4°C. The pellet was rehomogenized in an additional 4 ml of TES buffer using a Dounce homogenizer. Both

supernatants were combined for a total of 10 ml. Homogenate was centrifuged for 10 min at $100 \times g$ at 4°C . Supernatant was removed and the pellet was resuspended in 300- μl TES (input control). The supernatant was centrifuged again for 10 min at $5000 \times g$ at 4°C . The supernatant was removed and the pellet was resuspended in 300- μl TES to yield a plasma membrane enriched fraction.

IMMUNOBLOTTING. Protein concentration was determined using Quick Start Bradford Dye Reagent (500-0205, Bio-Rad). Proteins were transferred to polyvinylidene difluoride membranes and blocked in StartingBlock T20 Blocking Buffer; antibodies were also diluted in StartingBlock T20 Blocking Buffer (Pierce, Rockford, Illinois). Primary antibodies used were: SUR2 TMD1 (24), Glut4 (07-1404, Millipore), Glut1 (ab15309, Abcam, Cambridge, Massachusetts), GFP (MBL598), insulin receptor β (3025, Cell Signaling, Danvers, Massachusetts), dystrophin (NCL-DYSB; Leica Biosystems, Buffalo Grove, Illinois), Phospho-FoxO1 (Thr24)/FoxO3a (Thr32) (9464, Cell Signaling), FoxO1 (2880, Cell Signaling), AKT (4685, Cell Signaling), phosphorylated AKT Thr308 (9275S, Cell Signaling) and phosphorylated AKT Ser473 (9271, Cell Signaling). Secondary antibodies conjugated to horseradish peroxidase were used at 1:5,000 (Jackson ImmunoResearch Laboratories, West Grove, Pennsylvania). SuperSignal West Pico Chemiluminescent Substrate (Thermo Fisher Scientific, Rochester, New York) and a Fluor Chem E FE0538 documentation system (Protein Simple, San Jose, California) were used for imaging. MemCode (Thermo Fisher Scientific) reversible stain was used as a loading control for total transferred protein. Images were quantified from at least 3 mice per genotype using Fiji software (National Institutes of Health, Bethesda, Maryland) normalized against loading controls.

CO-REGULATION DATABASE. Meta-analysis of gene expression was performed on CO-Regulation Database.

GLUCOSE UPTAKE ASSAY. 2-Deoxyglucose (2DG) uptake was measured using a colorimetric assay kit (ab136955, Abcam). Isolated adult cardiomyocytes were plated in a 96-well plate at a density of 1,500 cells/well in 100 μl of Krebs Ringers Phosphate HEPES buffer (20-mM HEPES, 5-mM KH_2PO_4 , 1-mM MgSO_4 , 1-mM CaCl_2 , 136-mM NaCl, 4.7-mM KCl, pH 7.4) with 2% bovine serum albumin for 40 min. Cells were then treated with or without 1 mM of insulin for 20 min. Ten microliters of 10-mM 2DG were then added for 20 min. After 3 phosphate-buffered saline washes, the cells were harvested and 2DG was measured by colorimetric assay following the manufacturer's guidelines.

ISOLATED PERFUSED HEARTS FOR ^{13}C -GLUCOSE LABELING. Mice were anesthetized with inhaled 3% isoflurane and then euthanized with cervical dislocation, as described previously. Hearts were rapidly excised and placed in chilled heparinized modified Krebs-Henseleit buffer (118-mM NaCl, 4.7-mM KCl, 1.2-mM MgSO_4 , 1.2-mM KH_2PO_4 , 25-mM NaHCO_3 , 2.5-mM CaCl_2 , 0.5-mM EDTA, and 5-mM glucose). Extracardiac tissues were removed and discarded, and the aorta was cannulated with a 22-gauge cannula that was secured with 6-0 silk suture. Hearts were then perfused at a constant pressure of 80 mm Hg on a Langendorff apparatus with modified Krebs-Henseleit buffer equilibrated with 95% O_2 and 5% CO_2 at 37°C for 5 min. The media was then changed to ^{13}C -modified Krebs-Henseleit buffer containing 5 mM of ^{13}C -glucose in place of regular glucose. Hearts were perfused for 20 min followed by 5 min of washout with regular modified Krebs-Henseleit buffer. Hearts were then flash frozen.

METABOLITE ISOLATION. Flash frozen hearts from euthanized mice (metabolomic) or Langendorff apparatus (^{13}C -glucose labeling study) were powdered in a liquid nitrogen chilled mortar. One milliliter of methanol/water 80:20 (vol/vol) per sample was added. The homogenate was vortexed 1 min, and then centrifuge at $\sim 20,160 \times g$ for 15 min in a refrigerated centrifuge. Two hundred μl of supernatant was transferred into a tube with 800 μl of ice-cold methanol/water 80% (vol/vol). The protein pellet was used for protein quantitation using bicinchoninic acid assay. The metabolite-containing supernatant was then completely dried with a nitrogen gas N-EVAP (Organomation Associates, Inc. Berlin, Massachusetts). Dried metabolite pellets were conserved at -80°C until mass spectrometry processing.

MASS SPECTROMETRY. Services were performed by the Metabolomics Core Facility at Robert H. Lurie Comprehensive Cancer Center of Northwestern University. Fifty percent acetonitrile was added to the dried pellet tube for reconstitution, followed by centrifuged for 15 min at 20,000 g , 4°C . Supernatant was collected for liquid chromatography-mass spectrometry analysis. Samples were analyzed by high-performance liquid chromatography and high-resolution mass spectrometry and tandem mass spectrometry. The system uses a Thermo Q-Exactive in line with an electrospray source and an Ultimate3000 (Thermo Fisher Scientific) series high-performance liquid chromatography consisting of a binary pump, degasser, and auto-sampler outfitted with a Xbridge Amide column (Waters, Milford, Massachusetts) (dimensions of 4.6 mm \times 100 mm and

a 3.5- μ m particle size). The mobile phase A contained 95% (vol/vol) water, 5% (vol/vol) acetonitrile, 20-mM ammonium hydroxide, 20-mM ammonium acetate, pH 9.0; B was 100% acetonitrile. The gradient was as follows: 0 min, 15% acetonitrile; 2.5 min, 30% acetonitrile; 7 min, 43% acetonitrile; 16 min, 62% acetonitrile; 16.1 to 18 min, 75% acetonitrile; 18 to 25 min, 15% acetonitrile with a flow rate of 400 μ l/min. The capillary of the ESI source was set to 275°C, with sheath gas at 45 arbitrary units, auxiliary gas at 5 arbitrary units and the spray voltage at 4.0 kV. In positive-negative polarity switching mode, an m/z scan range from 70 to 850 was chosen and MS1 data were collected at a resolution of 70,000. The automatic gain control target was set at 1×10^6 and the maximum injection time was 200 ms. The top 5 precursor ions were subsequently fragmented, in a data-dependent manner, using the higher energy collisional dissociation cell set to 30% normalized collision energy in MS2 at a resolution power of 17,500. Data acquisition and analysis were carried out by Xcalibur 4.1 software and Tracefinder 4.1 software, respectively (Thermo Fisher Scientific).

GLYCOGEN MEASUREMENT. Glycogen storage was measured using a colorimetric assay kit (ab169558, Abcam) using 100,000 isolated adult cardiomyocytes boiled in 200 μ l of H₂O. The homogenate was processed following the manufacturer's guidelines.

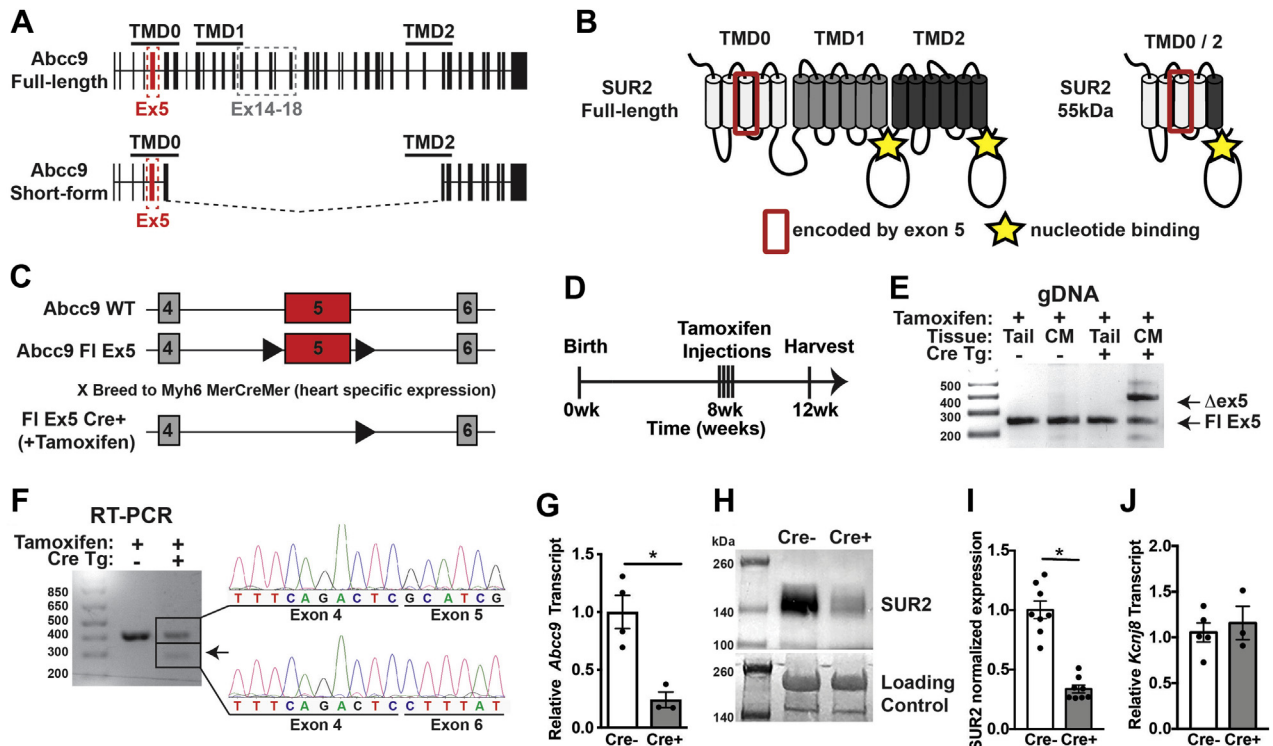
STATISTICAL ANALYSIS. Statistical analyses were performed with Prism 6 (GraphPad Software, La Jolla, California). Data were tested for significance using a 2-tailed Student's *t* test or using 2-way analysis of variance. Significance was determined as $p \leq 0.05$. Data are presented as single values overlaid on graphs of the mean \pm SEM. For the heart ischemia and reperfusion experiments, baseline data was compared using Prism and a Student's *t* test. Data was compared using a 2-way analysis of variance with Bonferroni's multiple comparisons test. The 2 cohorts that underwent ischemia protocols #1 and #2 were analyzed separately using a Student's *t* test.

RESULTS

TAMOXIFEN INDUCIBLE, CARDIAC-SPECIFIC DELETION OF *Abcc9*. Previously generated models of SUR2 mutations in mice resulted in distinct cardiovascular profiles. *Abcc9* mice engineered to lack exons 14 to 18, referred to as SUR2-Ex14/18 mice, survived but developed coronary artery spasm (13). This strategy resulted in global loss of full-length SUR2 but left intact the smaller splice form, SUR2-55 (Figures 1A and 1B). A second model, engineered to delete *Abcc9* exon 5 (SUR2-Ex5), ablated expression of

both full-length SUR2 and the smaller SUR2-55 (Figures 1A and 1B) (18). This model displayed a more profound cardiovascular outcome with neonatal cardiomyopathy and lethality by 3 weeks of age (models are summarized in Table 1). To selectively ablate SUR2 expression in the adult myocardium, we now generated a conditional *Abcc9* floxed exon 5 allele in which LoxP sites flanked exon 5 of *Abcc9*. This mouse was then crossed to a tamoxifen-inducible α MHC-MerCreMer (MCM) transgenic mouse for cardiomyocyte-specific deletion (Figure 1C) (19). Adult mice 8 weeks of age received tamoxifen for 4 consecutive days (Figure 1D). Tamoxifen exposure resulted in recombination of genomic DNA only in the presence of Cre recombinase in cardiomyocytes but not in genomic DNA isolated from tail tissue (Figure 1E). Sequencing of reverse transcriptase PCR products showed the expected deletion of exon 5 in MCM Cre+ hearts, while exon 5 was retained in MCM Cre- hearts (Figure 1F). Quantitative PCR showed >75% reduction in total *Abcc9* transcript in tamoxifen exposed MCM Cre+ hearts (Figure 1G). We hypothesize non-*Myh6* expressing fibroblasts and endothelial cells found within the whole heart are the main source of the remaining *Abcc9* transcript in MCM Cre+ samples. SUR2 protein levels correlated with the quantitative PCR findings, demonstrating >75% reduction in SUR2 levels in MCM Cre+ hearts (Figures 1H and 1I). Transcript levels from the *Kcnj8* gene, which is localized 16 Kb from the *Abcc9* gene, was similar between MCM Cre- and MCM Cre+ hearts by quantitative PCR (Figure 1J). Thus, tamoxifen-induced cardiac-specific Cre expression induced deletion of *Abcc9* exon 5 resulting in decreased *Abcc9* messenger RNA and SUR2 protein expression.

REDUCED BASELINE HEART FUNCTION IN CARDIAC SUR2-DELETED MICE. To examine the role of SUR2 in the adult myocardium, we analyzed hearts from mice at 4 weeks following tamoxifen treatment. Body weight from both female and male mice, as well as heart weight to body weight ratios were not significantly different between the 2 groups (Figures 2A and 2B). Unlike the globally deleted exon 5 mice, which die in the neonatal period, mice with cardiac specific deletion of SUR2 survived (Figure 2C) (18). M-mode echocardiography showed abnormal cardiac function in tamoxifen-treated MCM Cre+ hearts (Figure 2D). Cardiac SUR2-deleted mice exhibited significantly reduced systolic function, with fractional shortening of $35.9 \pm 1.8\%$ in the MCM Cre- and $27.5 \pm 1.9\%$ in the MCM Cre+ hearts (Figure 2E). No significant difference in diastolic left ventricular internal diameter or left ventricular posterior wall thickness was noted between groups

FIGURE 1 Selective Ablation of *Abcc9* in the Adult CM

(A) *Abcc9* encodes sulfonylurea receptor 2 (SUR2), the major SUR expressed in the myocardium. Shown is a schematic of *Abcc9*-produced transcripts encoding SUR2 full-length and SUR2-55KDa forms. Exon 5 is shown in red. (B) Shown is a depiction of full-length SUR2 containing 3 transmembrane domains (TMDs): TMD0, TMD1, and TMD2. SUR2-55KDa protein contains TMD0 and a portion of TMD2. The position of the protein domains encoded by exon 5 is shown with a red box. (C) *Abcc9* gene targeting of exon 5 with LoxP sites (black triangles) flanking exon 5 (red). These mice, referred to as FI Ex5 (floxed exon 5), were bred to mice carrying a transgene which expresses Cre recombinase under the control of the *Myh6* promoter, MerCreMer (MCM), creating the cardiac FI Ex5 mouse model (19). (D) Tamoxifen dosing strategy for deletion of *Abcc9* exon 5. (E) Polymerase chain reaction (PCR) of genomic deoxyribonucleic acid (DNA) isolated from tail clip or cardiomyocytes (CMs) from MCM Cre⁻ and MCM Cre⁺ FI Ex5 mice using a 3-primer strategy to detect the deletion of exon 5 (upper band) or floxed exon 5 (lower band). (F) Reverse transcriptase PCR (RT-PCR) from complementary DNA (cDNA) of tamoxifen-treated MCM Cre⁻ and MCM Cre⁺ mice show the exon 5-including transcript (upper band) and the transcript generated from the exon 5 deletion (lower band). Products confirmed by Sanger sequencing. (G) Quantitative PCR analysis of cDNA from ventricular myocardium from tamoxifen-treated MCM Cre⁻ and MCM Cre⁺ mice show reduced total *Abcc9* transcript levels in Cre⁺ mice (n = 4, 3; p = 0.008). (H, I) Immunoblot analysis of hearts from tamoxifen-treated MCM Cre⁻ and MCM Cre⁺ mice show reduction of full-length SUR2 protein (n = 8). *p < 0.001. (J) Quantitative PCR analysis of cDNA from isolated ventricular myocardium from tamoxifen-treated MCM Cre⁻ and MCM Cre⁺ mice show equal transcript levels of *Kcnj8* (n = 5, 3). gDNA = genomic DNA; Tg = transgenic; WT = wild-type.

(Figures 2F and 2G). These data showed that loss of SUR2 in adult cardiomyocytes was sufficient to induce a reduction in cardiac performance.

LOSS OF SUR2 PROVIDES RESISTANCE AGAINST ISOPROTERENOL-INDUCED CARDIAC FUNCTIONAL DECLINE. A 6-day course of twice daily injections of high-dose isoproterenol (200 mg/kg) has been shown to induce myocardial injury resulting in cardiac dysfunction with mild hypertrophic remodeling (21). To assess the effect of loss of SUR2 after in vivo cardiac injury and ventricular remodeling, MCM Cre⁺ and MCM Cre⁻ mice were injected repeatedly with isoproterenol to induce cardiac damage. Two days

following the final dose of isoproterenol, cardiac function was assessed through M-mode echocardiography (Figure 3A). Heart weight to body weight ratio was not significantly different between the 2 groups (Figure 3B). MCM Cre⁻ mice had reduced cardiac function after injury as evidenced by decreased percent fractional shortening, while MCM Cre⁺ mice did not show further deficit beyond the baseline decrease in fractional shortening (Figure 3C). Isoproterenol did not significantly alter diastolic left ventricular internal diameter in either group (Figure 3D). Left ventricular posterior wall thickness was modestly increased after isoproterenol challenge in both the MCM Cre⁺ and MCM Cre⁻ groups (Figure 3E).

TABLE 1 Summary of Genetic and Phenotypic Differences Among *Abcc9* Mouse Models

| Mouse Line | Ex 14/18 | Ex5 | FL Ex5 |
|--------------------|--|--|--|
| Genetic mutation | Deletion exons 14-18 | Deletion exon 5 | Floxed exon 5 |
| Isoforms expressed | Sur2-55 | – | – |
| Tissues affected | All | All | Myh6 Cre, cardiac specific |
| Survival | Survives to adulthood | Early lethality 14-21 days | Survives to adulthood |
| Phenotype | Cardiac vascular spasm, cardioprotection | Metabolic dysregulation, heart failure | Metabolic dysregulation, heart abnormalities, cardioprotection |
| Citation | Chutkow et al., 2001 (42) | Fahrenbach et al., 2014 (18) | This report |

Ex = exon; FL Ex5 = mice with LoxP sites flanking exon 5.

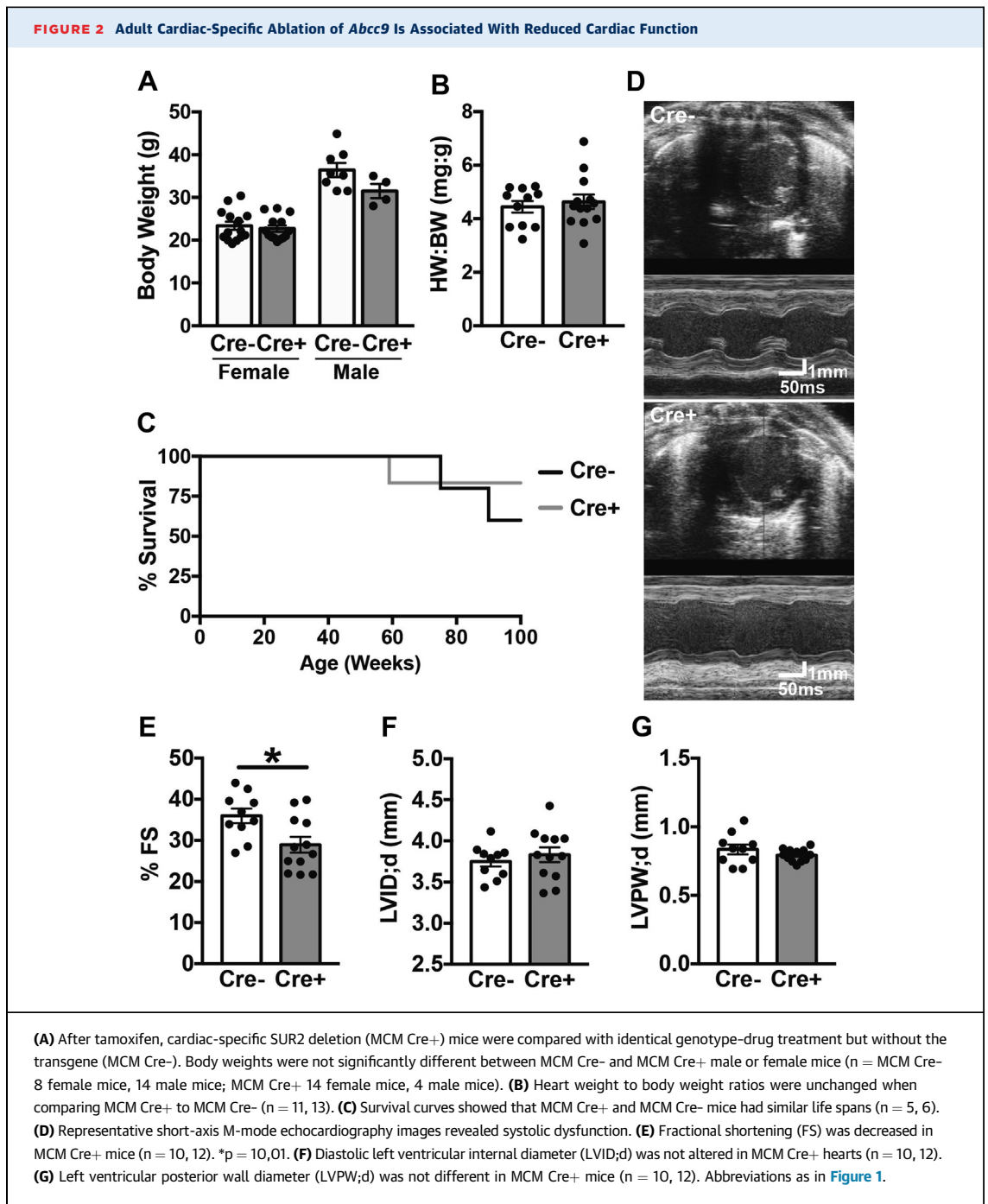
As expected, *Myh7* and *Nppa* mRNA expression measured by quantitative RT-PCR was increased in both MCM Cre- and MCM Cre in response to isoproterenol (Figure 3F). These results show that while loss of SUR2 in adult cardiomyocytes resulted in mildly depressed cardiac function, the SUR2-deleted hearts displayed resistance to isoproterenol-induced injury in vivo.

PRESERVED CARDIAC FUNCTION AND REDUCED INFARCT SIZE AFTER ISCHEMIA-REPERFUSION INJURY IN MCM Cre+ HEARTS. To further assess whether the loss of total SUR2 in the adult heart was cardioprotective during ischemic injury, MCM Cre+ and MCM Cre- hearts were subjected to ex vivo no-flow ischemia and reperfusion using a Langendorff constant pressure system. Maximum left ventricular developed pressure (LVDP) was decreased at baseline in MCM Cre+ mice (65.5 ± 4.0 mm Hg) compared with MCM Cre- (49.5 ± 2.0 mm Hg) (Figure 4A), consistent with baseline systolic impairment in MCM Cre+ hearts, while the percent recovery of LVDP following ischemia was significantly higher in MCM Cre+ hearts than control mice (Figure 4B). Correspondingly, at baseline, the maximal rate of pressure development was significantly decreased in tamoxifen-injected MCM Cre+ mice compared with MCM Cre- mice (Figure 4C). However, the percent recovery of the maximal rate of pressure development post-ischemia was significantly enhanced in cardiac SUR2-deleted hearts, showing a return to baseline, while the MCM Cre- hearts failed to return to baseline (Figure 4D). The maximal rate of pressure decline during relaxation was impaired at baseline in tamoxifen injected MCM Cre+ mice compared with MCM Cre- mice (Figure 4E). Again, a significantly improved percent recovery of the maximal rate of pressure decline during relaxation post-ischemia was seen in MCM Cre+ hearts compared with MCM Cre- control mice (Figure 4F). After both 30 or 45 min of global ischemia and 60 min of reperfusion, MCM Cre+ mice had significantly smaller infarct areas compared with

MCM Cre- control hearts (30 min: MCM Cre- 33 ± 6.3, MCM Cre+ 13.6 ± 1.2; 45 min: MCM Cre- 19.5 ± 4.5, MCM Cre+ 15.5 ± 2.7) (Figures 5A to 5C). These data indicate that, despite causing decreased baseline function, cardiac-specific loss of SUR2 was cardioprotective during ischemic injury.

GLUT4 COMPLEXES WITH SUR2. The findings of cardioprotection in the conditional cardiac SUR2 hearts prompted further analysis. The previously generated SUR2-Ex5 mice developed metabolic abnormalities, failing to fully transition to oxidative metabolism in early postnatal life (18). Using a CO-Regulation gene expression database (25), we queried genes that were concordantly expressed with *ABCC9*/SUR2. Among the list of genes highly co-expressed with *Abcc9* was *KCNJ8*, which encodes Kir6.1, a known partner protein of SUR2 (Table 2) (26). *SLC2A4*, which encodes the insulin-sensitive glucose transporter GLUT4, was >90% concordant with *ABCC9* expression (Table 2). The *Slc2a4* transcript and GLUT4 protein levels were not altered in cardiac SUR2-deleted hearts (Figures 6A and 6B). *Slc2a1*, which encodes GLUT1, and the GLUT1 proteins were also similarly unaffected by cardiac SUR2 ablation. To evaluate the possibility that GLUT4 and SUR2 interact, HEK cells were transfected with constructs to express GLUT4 with SUR2-GFP, SUR55-GFP, or KIR6.2-GFP. Co-immunoprecipitation with GLUT4 from HEK cell lysates showed that SUR2, SUR55, and KIR6.2 each co-associated with GLUT4 (Figure 6C). SUR2 also co-immunoprecipitated with GLUT4 in lysates prepared from normal hearts confirming that this interaction was present with natively expressed proteins (Figure 6D). These data indicated that SUR2 and GLUT4 interact, directly or indirectly, and may be in the same membrane complex.

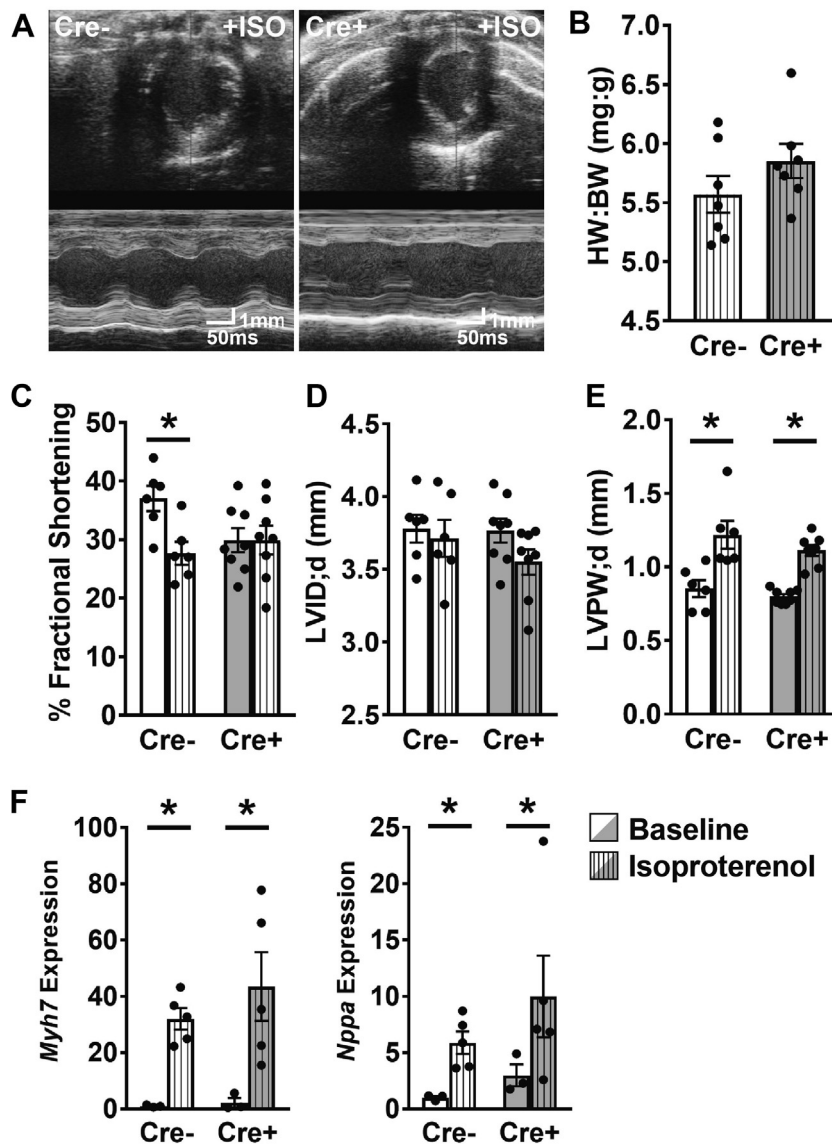
LOSS OF SUR2 ALTERS GLUCOSE UPTAKE AND GLUT4 LOCALIZATION. Translocation of GLUT4 to the sarcolemma increases glucose uptake by the cell and is directly stimulated by insulin signaling (27,28). To examine if the conditional deletion of SUR2 in



cardiomyocytes had functional implications in glucose handling, cardiomyocytes were isolated from MCM Cre- and MCM Cre+ floxed exon 5 mice and incubated with 2DG. 2DG is an analog of glucose that can be taken up by the cell but cannot be metabolized (29). With insulin exposure, both MCM Cre- and MCM Cre+ cardiomyocytes increased 2DG uptake ([Figure 7A](#)). However, SUR2-deleted cardiomyocytes

had greater 2DG uptake than those with intact SUR2, indicating enhanced insulin-stimulated glucose uptake in the absence of SUR2 ([Figure 7A](#)). We quantified GLUT4 in the plasma membrane of MCM Cre- and MCM Cre+ hearts 30 min after insulin stimulation and found a significant increase in membrane-enriched GLUT4 protein sampled from SUR2-deleted hearts ([Figure 7B](#)). The insulin receptor is a membrane

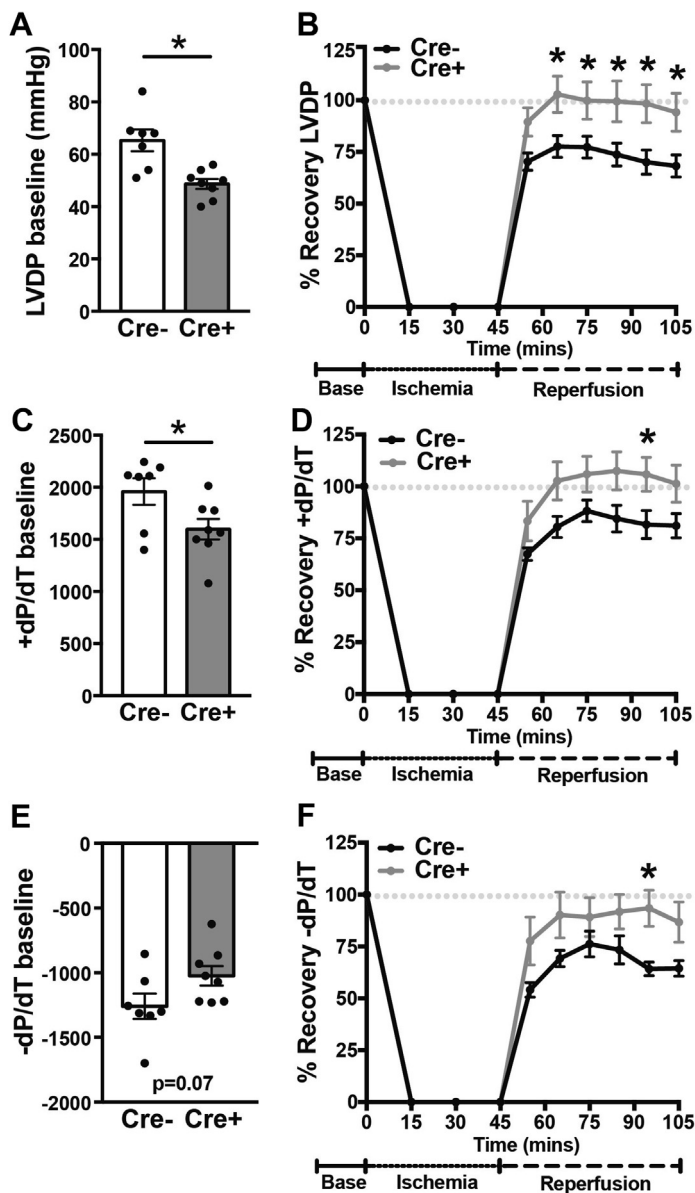
FIGURE 3 Loss of Cardiac *Abcc9* Mitigates Isoproterenol-Induced Cardiac Dysfunction



(A) Representative M-mode images of MCM Cre- and MCM Cre+ hearts were examined 2 days after the final isoproterenol injection. (B) Heart weight to body weight ratios showed no significant changes between genotypes (n = 7). (C) FS decreased with isoproterenol exposure in MCM Cre- mice while no reduction was noted in MCM Cre+ mice indicative of protection (n = 6, 8). *p = 0.03. (D) LVID;d was not altered in MCM Cre- or MCM Cre+ hearts with isoproterenol (n = 6, 8). (E) LVPW;d increased with isoproterenol exposure in both cohorts as expected (n = 6, 8). *p < 0.002. (F) Quantitative RT-PCR of hypertrophic markers *Myh7* and *Nppa* show both MCM Cre- and MCM Cre+ hearts showed the expected significant response to the isoproterenol challenge (n = 3, 5, 3, 5). *p = 0.04 *Myh7*, p = 0.001 *Nppa*. Abbreviations as in Figures 1 and 2.

protein that regulates glucose uptake by signaling through the AKT pathway, resulting in translocation of GLUT4-containing vesicles to the plasma membrane (30). Insulin receptor protein expression levels were similar in MCM Cre- and MCM Cre+ hearts (Figure 7C). However, the ratios of phosphorylated

AKT(Thr308) to total AKT and phosphorylated AKT(Ser473) to total AKT were significantly increased in SUR2-deleted hearts after insulin stimulation (Figures 7D and 7E). FOXO1 is a transcription factor that regulates energy metabolism, specifically increasing cardiac fatty acid uptake and inhibiting

FIGURE 4 Adult Cardiomyocyte-Specific Ablation of *Abcc9* Reduced Baseline Cardiac Performance But Enhanced Recovery After Ischemic Injury

Excised hearts, MCM Cre- and MCM Cre+, were subjected to 30 min of baseline measurement, followed by 45 min of no-flow ischemia, which was followed by 60 min of reperfusion. **(A)** Baseline left ventricular developed pressure (LVDP) was reduced in MCM Cre+ hearts, consistent with echocardiography data. *p = 0.002. **(B)** Following ischemia, MCM Cre+ hearts show improved recovery of LVDP compared with MCM Cre- hearts. *p < 0.02. **(C)** Baseline left ventricular maximal contractility (maximal rate of pressure development [+dP/dT]) was reduced in MCM Cre+ hearts. *p = 0.04. **(D)** Recovery of left ventricular maximal contractility +dP/dT was more efficient in MCM Cre+ hearts than in MCM Cre- hearts (*p = 0.04). **(E)** Baseline left ventricular maximal relaxation (maximal rate of pressure decline during relaxation [-dP/dT]) was reduced in Cre+ hearts. *p = 0.07. **(F)** Recovery of left ventricular maximal relaxation -dP/dT was more efficient in MCM Cre+ hearts than in MCM Cre- hearts (*p = 0.01). **(A to F)** n = 7, 8 hearts. Abbreviations as in [Figures 1 and 2](#).

glucose utilization (31-33). Moreover, the activity of FOXO is known to be negatively regulated through phosphorylation by AKT (34). We found the ratio of pFOXO1(Thr24)/FOXO1 was also significantly increased at baseline and after insulin stimulation in SUR2-deleted cardiomyocytes compared with controls ([Figure 7F](#)). These data show that in the absence of SUR2 there is an increase in insulin-dependent cardiac glucose uptake, an increase in GLUT4 in the membrane fraction and enhanced signaling. We conclude that this shift in glucose uptake can be adaptive in response to myocardial stress including isoproterenol infusion or infarct.

LOSS OF SUR2 ALTERS GLUCOSE UTILIZATION IN THE HEART AND LEADS TO INCREASED PHOSPHOCREATINE CONTENT.

The cardioprotection observed after ischemia reperfusion without circulating insulin, along with increased baseline insulin signaling in SUR2-deleted cardiomyocytes prompted us to better delineate cardiac metabolism in the absence of insulin using increased glucose uptake by both insulin and non-insulin dependent mechanisms. We profiled 115 hydrophilic metabolites (n = 3 hearts per group) ([Supplemental Table 2](#)). Phosphoenolpyruvate, a key metabolite of the glycolysis pathway, was significantly increased in MCM Cre+ hearts compared with MCM Cre- hearts ([Figure 8A](#)), and this was accompanied by a significant increase in phosphocreatine, an intracellular energy store ([Figure 8B](#)). Glycogen stores were not significantly different in the absence of SUR2/*Abcc9* ([Figure 8C](#)). These results indicate altered activity of either the consuming or producing reaction of phosphoenolpyruvate (35). To evaluate whether these findings reflected increased glycolysis, we performed a ¹³C-glucose labeling fractional enrichment on Langendorff-perfused hearts perfused with ¹³C-glucose for sufficient time to allow TCA cycle metabolite incorporation of ¹³C. The protocol included a wash-out with ¹²C-glucose to unmask possible differences in the rate of early glycolysis marked by ¹³C ([Figure 8D](#)). D-glyceraldehyde-3-phosphate and 3-phosphoglycerate showed a decrease in ¹³C incorporation in MCM Cre+ compared with MCM Cre-, as reflected by the mass distribution vector MDV ([Figure 8D](#)). ¹³C-pyruvate was differentially labeled between MCM Cre+ and MCM Cre- hearts. This result may be explained either by the duration of the washout time or by the different subcellular localization of pyruvate in the mitochondria versus cytoplasm. Interestingly ¹³C-alanine-3 incorporation, which reflects the level of mitochondrial pyruvate (36), was increased in the MCM Cre+ hearts, supporting increased mitochondrial pyruvate

production from glucose in the SUR2-deleted heart (Supplemental Figure 1). Tricarboxylic acid cycle metabolites showed no significant differences in these assays (Supplemental Figure 1). Three of the 4 metabolites measured were significantly different between MCM Cre⁺ and MCM Cre⁻ baseline hearts (Figure 8E). These data suggest altered glucose utilization in MCM Cre⁺ hearts and a low contribution of glucose in the TCA cycle.

DISCUSSION

REDUCED CARDIAC FUNCTION RELATED TO LOSS OF CARDIOMYOCYTE SUR2. Loss of SUR2 during development and in the neonatal window causes cardiomyopathy and death (18). The current investigation examined acute and chronic loss of SUR2 in the adult myocardium. This genetic deletion moderately reduced cardiac function but generated hearts that were partially protected from ischemia-reperfusion and isoproterenol insults. Cardiac-deleted SUR2 mice had smaller infarct sizes and less functional impairment after isoproterenol infusions. The degree of cardiac functional impairment at baseline was measurable but overall relatively modest in cardiac SUR2-deleted mice, and mice with deletion of SUR2 in the heart did not have shortened life spans. These findings are in contrast to mice carrying this same genetic deletion of exon 5 throughout development and in early postnatal life (18). In SUR2-Ex5 mice, a profound dilated cardiomyopathy developed in perinatal mice and correlated with demise, typically by 3 weeks of age. During early postnatal life, the mammalian heart undergoes a transition from glycolytic to oxidative metabolism as it adapts to high oxygen tension (37,38). Heart failure is similarly accompanied by a shift to glycolytic metabolism, and this state can be viewed as adaptive in the early stage, as the use of glucose requires less oxygen to generate the same amount of ATP (39). However, over the longer term, use of glucose leads to cardiac lipid accumulation and lipotoxicity, and thus becomes maladaptive (40). In contrast, the inability to use glucose in insulin-resistant diabetic hearts and associated diabetic cardiomyopathy is associated with excessive cardiomyocyte reactive oxidative species production by increasing fatty acid flux and oxidation (41). Those models exemplify the important balance of substrate utilization and plasticity in the healthy heart. Substrate prioritization, such as increase in glucose utilization, can provide short-term advantages under stress conditions, but become maladaptive in the long term. The decrease in left ventricular function seen in cardiac-deleted SUR2

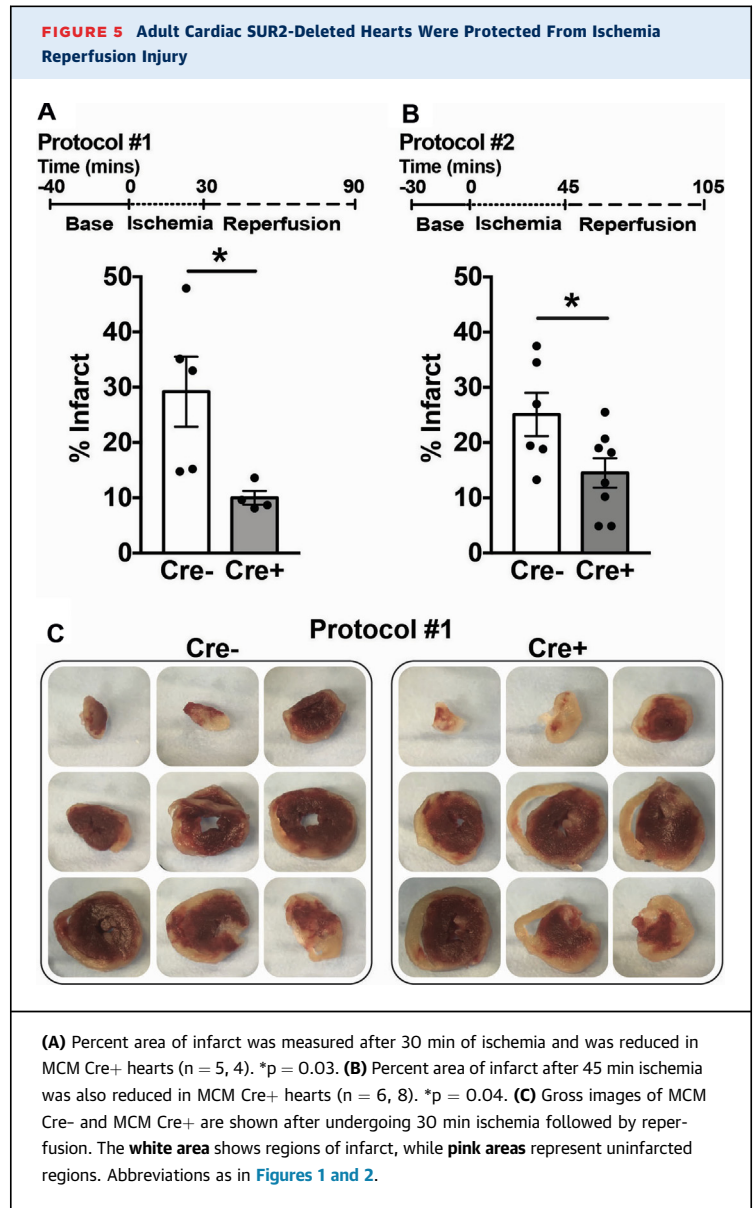
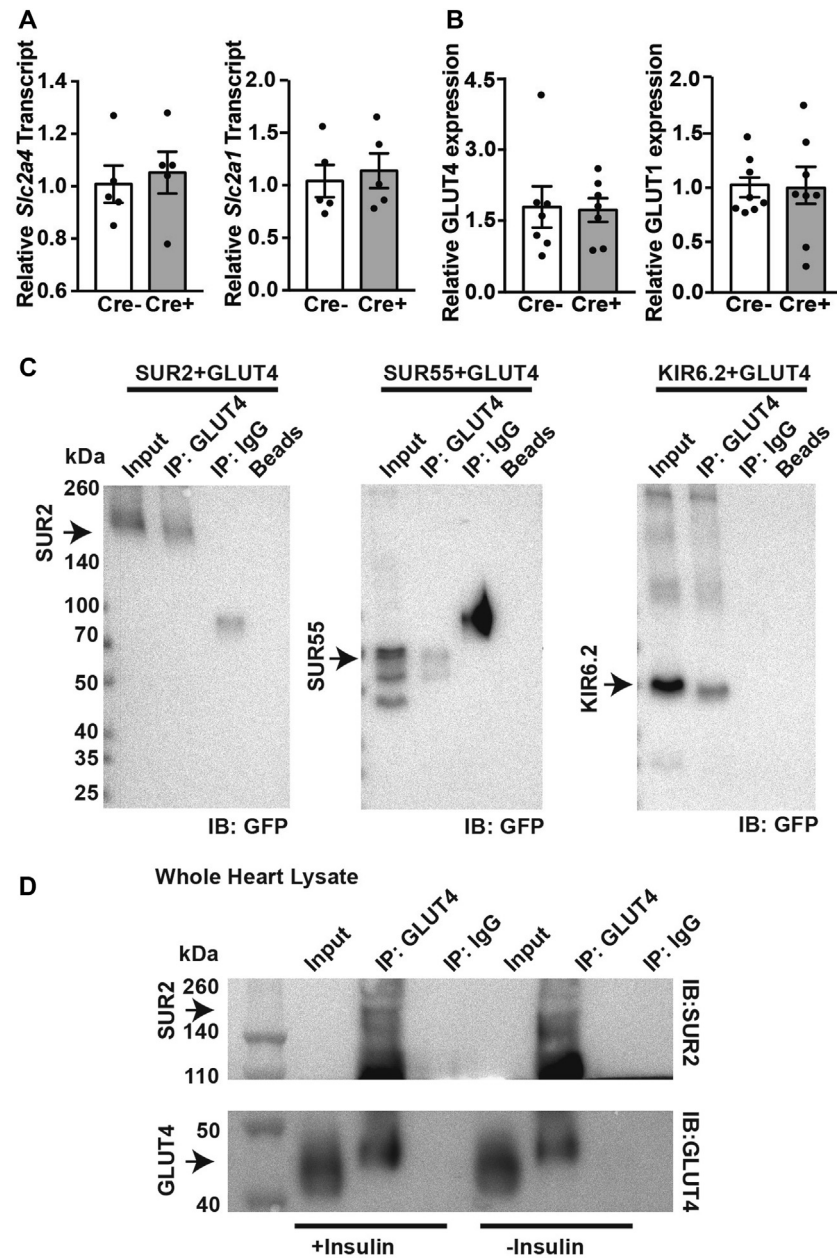


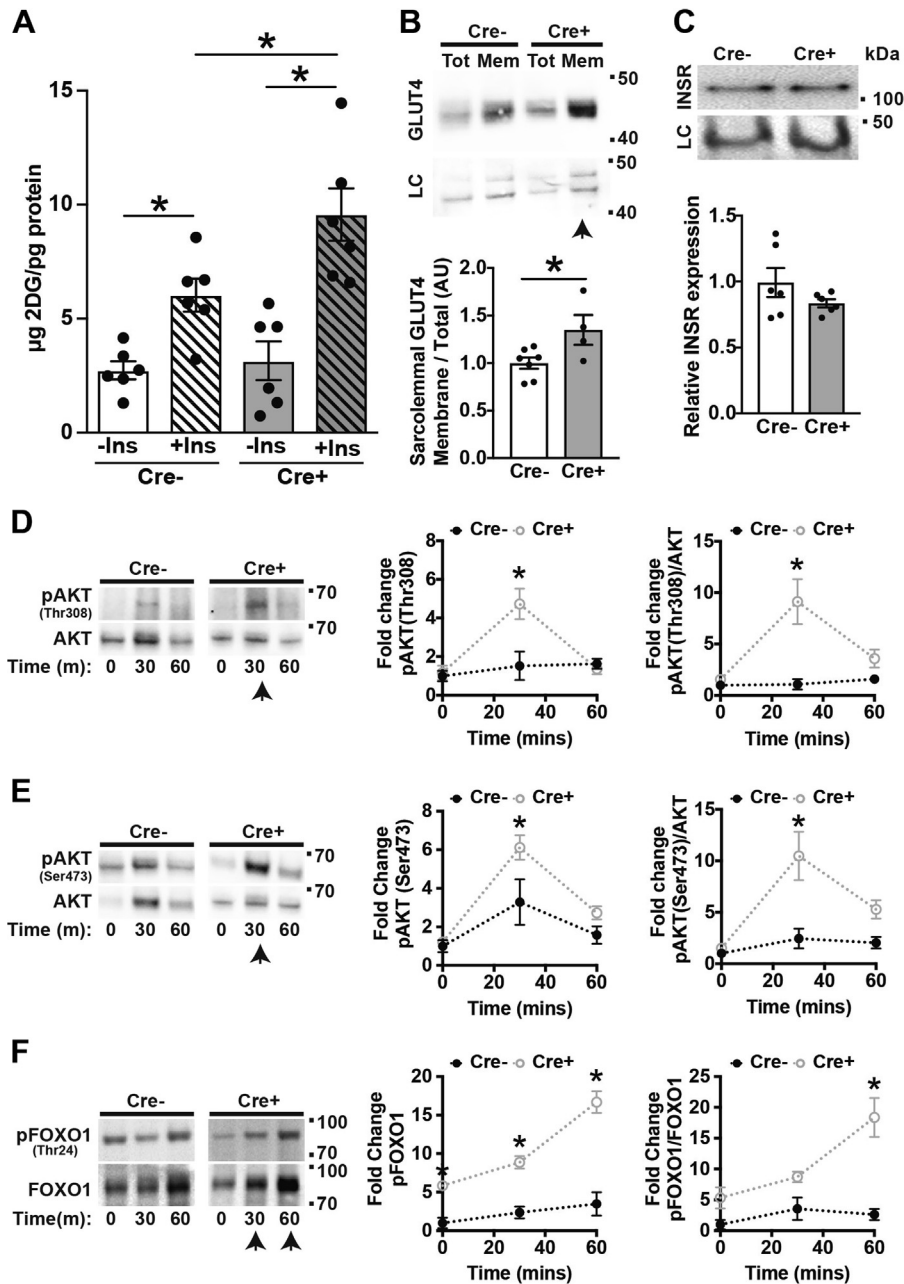
TABLE 2 CO-Regulation Database Analysis Shows Genes Concordantly Expressed With Abcc9

| Gene | Experiments With Abcc9 | Concordant (%) |
|--------|------------------------|----------------|
| ABRA | 95 | 98.9 |
| KCNJ8 | 403 | 98.5 |
| YIPF7 | 117 | 98.3 |
| ASB10 | 146 | 97.3 |
| TCAP | 194 | 91.7 |
| SMR2 | 142 | 91.5 |
| SLC2A4 | 331 | 91.2 |
| CSRP3 | 271 | 91.1 |
| NRAP | 303 | 91.1 |

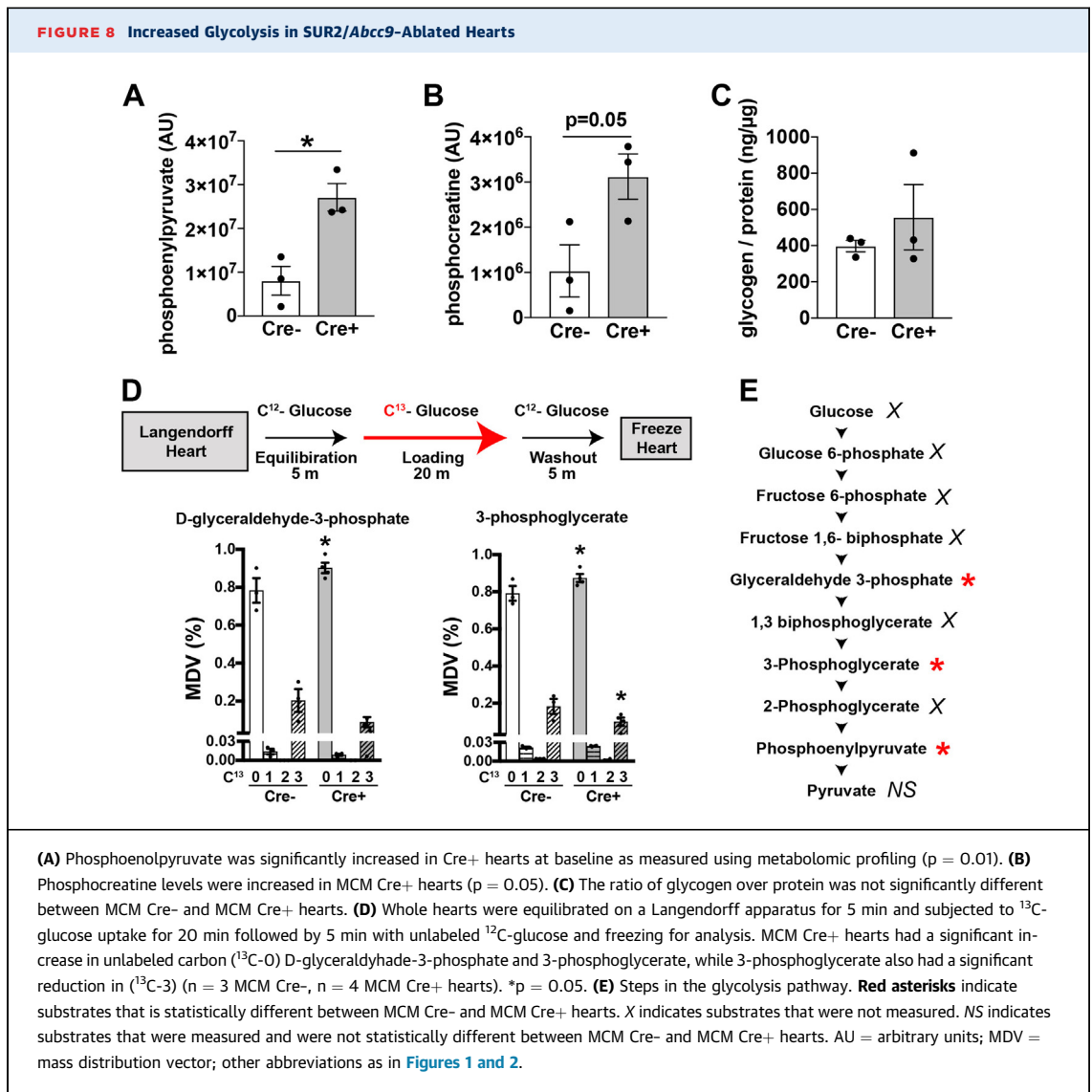
FIGURE 6 GLUT4 Is a SUR2-Interacting Protein

(A) Quantitative PCR analysis of cDNA of whole hearts from tamoxifen-treated Cre⁻ and Cre⁺ showed similar transcript levels of *Slc2a4*, which encodes glucose transporter 4 (GLUT4), and *Slc2a1*, which encodes GLUT1 ($n = 7$ per group). **(B)** Cre⁻ and Cre⁺ hearts express similar levels of GLUT4 and GLUT1 protein ($n = 7$ per group), as measured by quantitative immunoblotting. **(C)** SUR2, SUR55, and KIR6.2 each co-immunoprecipitated with GLUT4 when co-transfected in human embryonic kidney cells (arrows). Immunoprecipitation with immunoglobulin G (IgG) and beads alone did not result in co-immunoprecipitation and are shown as controls. **(D)** Full-length SUR2 is co-immunoprecipitated with GLUT4 from normal hearts, indicating this interaction occurs with native proteins. The interaction between GLUT4 and SUR2 was not altered in the presence of insulin. Immunoprecipitation (IP) with IgG is shown as a control. IB = immunoblot; GFP = green fluorescent protein; other abbreviations as in [Figures 1 and 2](#).

FIGURE 7 SUR2 Regulates Glucose Uptake and GLUT4 Localization in Adult Hearts



(A) Insulin stimulation significantly increased 2-deoxyglucose (2DG) uptake in both MCM Cre- and MCM Cre+ cardiomyocytes. 2DG levels were significantly elevated in MCM Cre+ cardiomyocytes compared with MCM Cre- cardiomyocytes post-insulin stimulation ($n > 7$). $*p < 0.05$. (B) Thirty minutes post-insulin injection MCM Cre+ hearts showed increased GLUT4 in the plasma membrane fraction of prepared microsomes (black arrow) ($n \geq 4$ per genotype). Total protein was used as a loading control (LC). Relative sarcolemmal GLUT4 is represented as the ratio of membrane fraction GLUT4 over total GLUT4. $*p < 0.03$. (C) Insulin receptor (INSR) protein levels were unchanged between MCM Cre- and MCM Cre+ hearts ($n = 6$); LC, loading control. (D, E) Thirty min post-insulin injection MCM Cre+ hearts showed a significant elevation (black arrow) in the ratio of phosphorylated AKT (pAKT) (Thr308)/AKT and phosphorylated AKT(Ser473)/AKT ($n = 4$). $*p < 0.001$ Thr308, $*p = 0.003$ Ser473. (F) Thirty and 60 min post-insulin injection, MCM Cre+ hearts showed a significant elevation in the ratio of phosphorylated FOXO1 (pFOXO1) (Thr24)/FOXO1 (black arrows) ($n = 4$). $*p < 0.0001$. -Ins = without insulin; +Ins = plus insulin; AU = arbitrary units; other abbreviations as in Figures 1 and 2.



hearts at baseline is consistent with these same observations; however, this decrease of cardiac function was not associated with a shortened life span.

IMPROVED ADAPTATION TO SHORT-TERM STRESSORS. Strikingly, we observed that adult cardiac-deleted SUR2 hearts were able to withstand short-term cardiac stressors better than normal counterparts. Specifically, 2 different methods, high-dose isoproterenol infusion and ischemia reperfusion, showed that adult cardiac-deleted SUR2 hearts maintained function better after these insults. These findings suggest that the metabolic shift resulting from loss of SUR2 makes cardiomyocytes more resilient to acute stress. We expect that longer-term stressors would more adversely affect hearts lacking SUR2, as glucose utilization is less able to maintain

energy supplies. We previously observed that SUR2 Ex14-18 hearts developed vascular spasm (13) and hypothesized that vascular spasm in this setting effectively pre-conditioned the myocardium, rendering it more likely to adapt to ischemic insult (15). We examined cardiac-deleted SUR2 for any evidence of vascular spasm using telemetry to look for ST-segment elevation but did not observe this (Supplemental Figure 2). The current model demonstrates that the loss of SUR2 in the cardiomyocyte itself is responsible for adaptation to short-term stressors.

INCREASED INSULIN SIGNALING IN CARDIOMYOCYTE-SUR2 HEARTS. We previously observed that SUR2 Ex14-18 skeletal muscle had increased glucose uptake despite no change in GLUT4 expression (42). In this study, we now found that SUR2-deleted hearts show

increased glucose uptake and utilization through at least 2 distinct mechanisms. First, GLUT4, the major insulin-sensitive transporter in the heart was found in a complex with SUR2. Co-expression of SUR1 and GLUT4 has been noted in some cell types (43). Both SUR2 and GLUT4 are enriched in striated muscles, including both cardiac and skeletal muscle. GLUT4 is dynamic and recruited to and from the plasma membrane in response to insulin (44,45). Consistent with this, we identified excessive glucose uptake in cardiomyocytes lacking SUR2. These data are consistent with a model where GLUT4 internalization and recycling may be delayed, leading to excessive glucose uptake, which alters glucose handling and energy storage as phosphocreatine. Secondly, we show that insulin signaling was increased in cardiac-deleted SUR2 hearts, reflected by an increase in AKT phosphorylation and activation of downstream targets such as FOXO.

Taken together, excessive glucose uptake into the myocardium, mediated by loss of SUR2 in cardiomyocytes, leads to reduced cardiac function and altered handling of glucose in this model that correlates with a cardioprotective metabolic and bioenergetic milieu. This increase in glucose uptake was

accompanied by enhanced insulin signaling. Loss of SUR2 in cardiomyocytes and the resulting metabolic shifts generates a myocardium that is resistant to cardiac stress.

ADDRESS FOR CORRESPONDENCE: Dr. Elizabeth M. McNally, Northwestern University Feinberg School of Medicine, Center for Genetic Medicine, 303 East Superior Street, Lurie 7-123, Chicago, Illinois 60611. E-mail: elizabeth.mcnally@northwestern.edu.

PERSPECTIVES

COMPETENCY IN MEDICAL KNOWLEDGE: Sulfonylurea receptor antagonists remain in use to treat diabetes mellitus since they are largely effective. The cardiovascular safety of the sulfonylureas has been debated. Most commonly used sulfonylurea receptor agonists have greater affinity for SUR1, which is expressed in the pancreatic beta cell, compared with their affinity for SUR2.

TRANSLATIONAL OUTLOOK: The presence of agents that react with SURs indicates that these agents can be targeted and, in doing so, may offer a path to protecting the myocardium.

REFERENCES

1. Noma A. ATP-regulated K⁺ channels in cardiac muscle. *Nature* 1983;305:147-8.
2. Flagg TP, Enkvetchakul D, Koster JC, Nichols CG. Muscle KATP channels: recent insights to energy sensing and myoprotection. *Physiol Rev* 2010;90:799-829.
3. Kefaloyianni E, Bao L, Rindler MJ, et al. Measuring and evaluating the role of ATP-sensitive K⁺ channels in cardiac muscle. *J Mol Cell Cardiol* 2012;52:596-607.
4. Rubaiy HN. The therapeutic agents that target ATP-sensitive potassium channels. *Acta Pharm* 2016;66:23-34.
5. Zingman LV, Hodgson DM, Bast PH, et al. Kir6.2 is required for adaptation to stress. *Proc Natl Acad Sci U S A* 2002;99:13278-83.
6. Liu XK, Yamada S, Kane GC, et al. Genetic disruption of Kir6.2, the pore-forming subunit of ATP-sensitive K⁺ channel, predisposes to catecholamine-induced ventricular dysrhythmia. *Diabetes* 2004;53 Suppl 3:S165-8.
7. Tokuyama Y, Fan Z, Furuta H, et al. Rat inwardly rectifying potassium channel Kir6.2: cloning, electrophysiological characterization, and decreased expression in pancreatic islets of male Zucker diabetic fatty rats. *Biochem Biophys Res Comm* 1996;220:532-8.
8. Chutkow WA, Simon MC, Le Beau MM, Burant CF. Cloning, tissue expression, and chromosomal localization of SUR2, the putative drug-binding subunit of cardiac, skeletal muscle, and vascular KATP channels. *Diabetes* 1996;45:1439-45.
9. Ashford MLJ, Bond CT, Blair TA, Adelmair JP. Cloning and functional expression of a rat heart KATP channel. *Nature* 1994;370:456-9.
10. Clement JP, Kunjilwar K, Gonzalez G, et al. Association and stoichiometry of KATP channel subunits. *Neuron* 1997;18:27-38.
11. Kane GC, Behfar A, Dyer RB, et al. KCNJ11 gene knockout of the Kir6.2 KATP channel causes maladaptive remodeling and heart failure in hypertension. *Hum Mol Genet* 2006;15:2285-97.
12. Kane GC, Lam CF, O'Clohain F, et al. Gene knockout of the KCNJ8-encoded Kir6.1 K(ATP) channel imparts fatal susceptibility to endotoxemia. *FASEB J* 2006;20:2271-80.
13. Chutkow WA, Pu J, Wheeler MT, et al. Episodic coronary artery vasospasm and hypertension develop in the absence of Sur2 K(ATP) channels. *J Clin Invest* 2002;110:203-8.
14. Miki T, Suzuki M, Shibasaki T, et al. Mouse model of Prinzmetal angina by disruption of the inward rectifier Kir6.1. *Nat Med* 2002;8:466-72.
15. Stoller D, Kakkar R, Smelley M, et al. Mice lacking sulfonylurea receptor 2 (SUR2) ATP-sensitive potassium channels are resistant to acute cardiovascular stress. *J Mol Cell Cardiol* 2007;43:445-54.
16. Shi N-Q, Ye B, Makielski JC. Function and distribution of the SUR isoforms and splice variants. *J Mol Cell Card* 2005;39:51-60.
17. Pu J-L, Ye B, Kroboth SL, McNally EM, Makielski JC, Shi N-Q. Cardiac sulfonylurea receptor short form-based channels confer a glibenclamide-insensitive KATP activity. *J Mol Cell Card* 2008;44:188-200.
18. Fahrenbach JP, Stoller D, Kim G, et al. Abcc9 is required for the transition to oxidative metabolism in the newborn heart. *FASEB J* 2014;28:2804-15.
19. Sohal DS, Nghiem M, Crackower MA, et al. Temporally regulated and tissue-specific gene manipulations in the adult and embryonic heart using a tamoxifen-inducible Cre protein. *Circ Res* 2001;89:20-5.
20. Barefield DY, Puckelwartz MJ, Kim EY, et al. Experimental modeling supports a role for MyBP-HL as a novel myofibrillar component in arrhythmia and dilated cardiomyopathy. *Circulation* 2017;136:1477-91.
21. Wallner M, Duran JM, Mohsin S, et al. Acute catecholamine exposure causes reversible myocyte injury without cardiac regeneration. *Circ Res* 2016;119:865-79.
22. Fuller W, Eaton P, Medina RA, Bell J, Shattock MJ. Differential centrifugation separates cardiac sarcolemmal and endosomal membranes from Langendorff-perfused rat hearts. *Anal Biochem* 2001;293:216-23.
23. Tepavcevic S, Koricanac G, Zakula Z, Milosavljevic T, Stojiljkovic M, Isenovic ER. Interaction between insulin and estradiol in regulation of cardiac glucose and free fatty acid transporters. *Horm Metab Res* 2011;43:524-30.

24. Kakkar R, Ye B, Stoller DA, et al. Spontaneous coronary vasospasm in KATP mutant mice arises from a smooth muscle-extrinsic process. *Circ Res* 2006;98:682-9.
25. Fahrenbach JP, Andrade J, McNally EM. The CO-Regulation Database (CORD): a tool to identify coordinately expressed genes. *PLoS One* 2014;9:e90408.
26. Bryan J, Munoz A, Zhang X, et al. ABCC8 and ABCC9: ABC transporters that regulate K⁺ channels. *Pflugers Arch* 2007;453:703-18.
27. Saltiel AR, Kahn CR. Insulin signalling and the regulation of glucose and lipid metabolism. *Nature* 2001;414:799-806.
28. Bryant NJ, Govers R, James DE. Regulated transport of the glucose transporter GLUT4. *Nat Rev Mol Cell Biol* 2002;3:267-77.
29. Yamamoto N, Ueda M, Sato T, et al. Measurement of glucose uptake in cultured cells. *Curr Protoc Pharmacol* 2011. Chapter 12:Unit 12.14.1-22.
30. Leto D, Saltiel AR. Regulation of glucose transport by insulin: traffic control of GLUT4. *Nat Rev Mol Cell Biol* 2012;13:383-96.
31. Ronnebaum SM, Patterson C. The FoxO family in cardiac function and dysfunction. *Annu Rev Physiol* 2010;72:81-94.
32. Chistiakov DA, Orekhov AN, Bobryshev YV. The impact of FOXO-1 to cardiac pathology in diabetes mellitus and diabetes-related metabolic abnormalities. *Int J Cardiol* 2017;245:236-44.
33. Xin Z, Ma Z, Jiang S, et al. FOXOs in the impaired heart: new therapeutic targets for cardiac diseases. *Biochim Biophys Acta* 2017;1863:486-98.
34. Brown AK, Webb AE. Regulation of FOXO factors in mammalian cells. *Curr Top Dev Biol* 2018;127:165-92.
35. Buescher JM, Antoniewicz MR, Boros LG, et al. A roadmap for interpreting (13)C metabolite labeling patterns from cells. *Curr Opin Biotechnol* 2015;34:189-201.
36. Groen AK, Wanders RJ, Westerhoff HV, van der Meer R, Tager JM. Quantification of the contribution of various steps to the control of mitochondrial respiration. *J Biol Chem* 1982;257:2754-7.
37. Warsaw JB. Cellular energy metabolism during fetal development. IV. Fatty acid activation, acyl transfer and fatty acid oxidation during development of the chick and rat. *Dev Biol* 1972;28:537-44.
38. Piquereau J, Novotova M, Fortin D, et al. Postnatal development of mouse heart: formation of energetic microdomains. *J Physiol* 2010;588:2443-54.
39. Azevedo PS, Minicucci MF, Santos PP, Paiva SA, Zornoff LA. Energy metabolism in cardiac remodeling and heart failure. *Cardiol Rev* 2013;21:135-40.
40. van der Vusse GJ, Glatz JF, Stam HC, Reneman RS. Fatty acid homeostasis in the normoxic and ischemic heart. *Physiol Rev* 1992;72:881-940.
41. Shah MS, Brownlee M. Molecular and cellular mechanisms of cardiovascular disorders in diabetes. *Circ Res* 2016;118:1808-29.
42. Chutkow WA, Samuel V, Hansen PA, et al. Disruption of Sur2-containing K(ATP) channels enhances insulin-stimulated glucose uptake in skeletal muscle. *Proc Natl Acad Sci U S A* 2001;98:11760-4.
43. Yee KK, Sukumaran SK, Kotha R, Gilbertson TA, Margolskee RF. Glucose transporters and ATP-gated K⁺ (KATP) metabolic sensors are present in type 1 taste receptor 3 (T1r3)-expressing taste cells. *Proc Natl Acad Sci U S A* 2011;108:5431-6.
44. Abel ED. Glucose transport in the heart. *Front Biosci* 2004;9:201-15.
45. Steinbusch LK, Schwenk RW, Ouwens DM, Diamant M, Glatz JF, Luiken JJ. Subcellular trafficking of the substrate transporters GLUT4 and CD36 in cardiomyocytes. *Cell Mol Life Sci* 2011;68:2525-38.

KEY WORDS ABCC9, ischemia, potassium ATP channels, sulfonylurea

APPENDIX For supplemental tables and figures, please see the online version of this paper.